# Role of electron-phonon scattering on the vacuum Rabi splitting of a single-quantum dot and a photonic crystal nanocavity

F. Milde* and A. Knorr
*Institut für Theoretische Physik, Nichtlineare Optik und Quantenelektronik, Technische Universität Berlin, Hardenbergstraße 36, PN 7-1 10623 Berlin, Germany*

S. Hughes
*Department of Physics, Queen's University, Kingston, Ontario, Canada K7L 3N6*
(Received 30 October 2007; revised manuscript received 28 April 2008; published 25 July 2008)

We study the influence of non-Markovian electron-acoustic-phonon scattering on the vacuum Rabi splitting of a semiconductor single-quantum dot and a planar photonic crystal nanocavity. The regimes of strong coupling and side-coupled light transmission are explored as a function of temperature. At elevated temperatures, when the quantum dot has left the strong-coupling regime, a spectral splitting continues to be observed in transmission. The effects of non-Markovian scattering are shown to significantly vary the characteristic transmissivity compared to purely model Lorentzian line shapes for the electron-phonon interaction.

DOI: 10.1103/PhysRevB.78.035330 PACS number(s): 78.67.Hc, 63.22.−m, 41.20.Jb, 42.55.Tv

## I. INTRODUCTION

Planar photonic crystal (PC) nanocavities (NCs) formed by spatial defects possess large quality factors ($Q>10^6$) and low effective mode volumes ($V\sim 0.05\ \mu m^3$) as shown by Akahane *et al.*[1] for a Si-based structure. These large $Q/V$-ratio cavities are important for studying fundamental cavity-quantum electrodynamics (cQED) and for applications in quantum information science using compact solid-state devices. Recently, single semiconductor quantum dot (QD) vacuum Rabi splitting[2] and the deterministic coupling of QDs to PC nanocavities have been realized.[3,4] It has also been predicted that the integration of PC waveguides (WGs) into such photonic structures allows one to modify the propagation of light that is side coupled to a QD within a NC, yielding signatures of vacuum Rabi splitting[5] and dipole-induced transparency.[6]

While these complex nanophotonic regimes have been theoretically discussed using simplified light-matter interaction theories with two-level emitters, a comprehensive understanding of the photonic coupling effects requires the inclusion of decoherence and scattering effects induced by the surrounding media. A typical example is the quantum confined electron-hole pair coherence in QDs interacting with acoustical phonons at elevated temperatures. While QDs in microcavities in the absence of electron-phonon scattering[7,8] and the basic influence of electron-phonon scattering for single QDs in a homogeneous semiconductor environment[9–13] are well understood, only a few works on the impact of electron-phonon interaction on QDs in nanocavities exist.[14,15] Despite these works, where phonons are treated by either (polaron Green functions and) spectral density functions[14] or on a level of a phase diffusion model,[15] the precise role of temperature on QD emission in PC structures remains unknown. In this work, we investigate the impact of an acoustical phonon bath on the transmission spectra of a NC containing a QD side coupled to a PC waveguide. By employing the independent Boson model (IBM) (Refs. 10–12 and 16) for the electron-phonon interaction, coupled to a photon Green function technique to include the PC, a numerically exact solution within a semiclassical theory is found.

## II. WAVEGUIDE FIELD TRANSMISSION

We first introduce the essential formulas to describe the transmission spectra of a planar PC WG coupled to a NC, including a semiconductor QD. The photonic structure that we study is shown schematically in Fig. 1. The planar PC is made up of air holes in a dielectric semiconductor medium and the WG is formed by a one-dimensional (1D) line defect of missing holes. This leads to a defect mode in the photonic band structure, which lies within the photonic band gap. The WG modes of interest do not couple to the continuum of radiation states above the light line and hence light can be transmitted through the structure almost lossless (neglecting disorder-induced *extrinsic* scattering[17]). In close proximity we find a point defect where the electromagnetic field is spatially located (confined) and so forms a NC. Due to the spatial overlap between waveguide and nanocavity modes, $\mathbf{E}_{WG}(\mathbf{r})$ and $\mathbf{E}_{NC}(\mathbf{r})$, the latter can couple into the WG. When placing a QD inside the NC, significant changes in the optical behavior occur.

The emission properties of a complex photonic environment can be described within a Green function tensor (GFT)

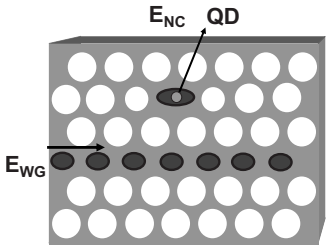


FIG. 1. Top view for a PC waveguide including a side-coupled QD embedded within a NC; $\mathbf{E}_{NC}$ and $\mathbf{E}_{WG}$ denote the cavity and propagating waveguide modes.

 

formalism.[18] The GFT $\mathbf{G}(\mathbf{r},\mathbf{r}',\omega)$ corresponds to the $\mathbf{E}$ field response at $\mathbf{r}'$ to an oscillating dipole at $\mathbf{r}$ as a function of frequency $\omega$. The solutions for the electric-field propagation through the nanostructure can be written in terms of the GFT that satisfies $[\nabla\times\nabla\times-\omega^2/c^2\varepsilon(\mathbf{r},\omega)]\mathbf{G}(\mathbf{r},\mathbf{r}',\omega)=\omega^2/c^2\mathbf{1}\delta(\mathbf{r}-\mathbf{r}')$, with $\mathbf{1}$ as the unit tensor. Following Ref. 5 with a given susceptibility $\varepsilon(\mathbf{r},\omega)$ (including the PC, WG, and NC), the solution for the GFT can be found by expanding $\mathbf{G}$ into the cavity and waveguide modes of the system, $\mathbf{E}_{\mathrm{NC}}$ and $\mathbf{E}_{\mathrm{WG}}$. One obtains $\mathbf{G}=\mathbf{K}-\delta(\mathbf{r}-\mathbf{r}')/\varepsilon(\mathbf{r},\omega)$, where $\mathbf{K}=\Sigma_{\mathbf{k}}\omega_{\mathbf{k}}^2/(\omega_{\mathbf{k}}^2-\omega^2)\mathbf{E}_{\mathbf{k}}^T(\mathbf{r})\otimes\mathbf{E}_{\mathbf{k}}^T(\mathbf{r}')$; the modified GFT $\mathbf{K}$ includes only quasitransverse modes and avoids divergences in $\mathrm{Re}[\mathbf{G}(\mathbf{r},\mathbf{r},\omega)]$ while, under the assumption of a real valued susceptibility $\varepsilon(\mathbf{r},\omega)$, the identity $\mathrm{Im}[\mathbf{G}(\mathbf{r},\mathbf{r}',\omega)]=\mathrm{Im}[\mathbf{K}(\mathbf{r},\mathbf{r}',\omega)]$ holds.[19,20] It is also presumed that the WG and NC resonances are spectrally located deep inside the photonic band gap of the PC and that they are weakly coupled to each other. For the WG and NC under consideration, the weak-coupling assumption is justified since one usually seeks to maximize $Q$. This scenario insures that the signal transmitted through the waveguide represents the response of the NC or, if the QD is added, the vacuum Rabi splitting signal of the NC and QD.

To derive the corresponding transmission spectra, a NC without a QD but side coupled to the WG is considered first. Given by the amplitude ratio of the field (polarization direction unit vector $\mathbf{e}_{\mathbf{k}}$) far right of the cavity and the injected forward propagating WG mode, the complex frequency-dependent transmission coefficient $t(\omega)$ is obtained, $t(\omega)=\mathbf{E}(x\to+\infty)\cdot\mathbf{e}_{\mathbf{k}}/\mathbf{E}_{\mathrm{WG}}^{\mathbf{k}_\omega}(x\to+\infty)\cdot\mathbf{e}_{\mathbf{k}}$. This leads to[5]

$$t(\omega)=1+\frac{i\omega\Gamma_{\mathrm{NC}}(\omega)}{\omega_{\mathrm{NC}}^2-\omega^2-i\omega[\Gamma_{\mathrm{NC}}(\omega)+\Gamma_{\mathrm{NC}}^0]},\tag{1}$$

where $\omega_{\mathrm{NC}}$ is the cavity resonance frequency and $\Gamma_{\mathrm{NC}}^0$ is the bare mode decay rate accounting for intrinsic out-of-plane scattering. Additionally, $\Gamma_{\mathrm{NC}}(\omega)$ is the coupling rate between the waveguide and cavity modes. For vanishing coupling, the WG transmission is one. For planar PCs, typically $\Gamma_{\mathrm{NC}}$ is much larger than the bare $\Gamma_{\mathrm{NC}}^0$. Since the quality factor of a cavity is, in general, defined as $Q=(\text{cavity frequency})/(\text{cavity linewidth})$, we will, consistently with experiments,[21] employ the two distinct quality factors $\Gamma_{\mathrm{NC}}=\omega_{\mathrm{NC}}/Q_c$ and $\Gamma_{\mathrm{NC}}^0=\omega_{\mathrm{NC}}/Q_0$ instead of calculating $\Gamma_{\mathrm{NC}}$ explicitly. Thus Eq. (1) has a typical Lorentzian oscillator line shape [cf. solid curve in Fig. 2(b)]. We now consider a QD that is embedded into the NC. By exploiting a Dyson equation for the GFT of the QD,[5] we derive a modified transmission coefficient:

$$t(\omega)=1+\frac{i\omega\Gamma_{\mathrm{NC}}[1+V_d\Delta\varepsilon_d^{\mathrm{re}}(\omega)\mathbf{n}_d\cdot\mathbf{K}(\mathbf{r}_d,\mathbf{r}_d,\omega)\cdot\mathbf{n}_d]}{\omega_{\mathrm{NC}}^2-\omega^2-i\omega(\Gamma_{\mathrm{NC}}+\Gamma_{\mathrm{NC}}^0)},\tag{2}$$

with the renormalized QD susceptibility $\Delta\varepsilon_d^{\mathrm{re}}$, which accounts for the radiation self-energy of the QD within the complete photonic structure, given by

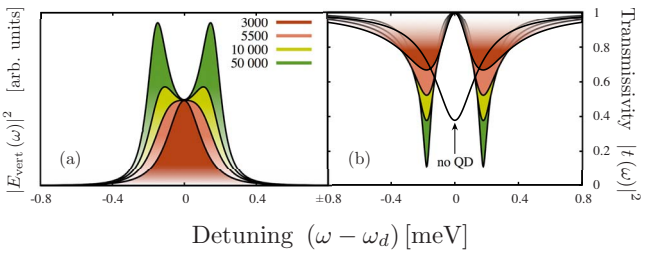


FIG. 2. (Color online) Vacuum Rabi splitting in the (a) vertically scattered light and (b) transmissivity of a single QD (dipole moment $d_{12}=50$ D: $\approx 1$ e nm) on resonance with a cavity ($Q_c=6000$). Shown are results for decreasing mode decay rate $\Gamma_{\mathrm{NC}}^0$, i.e., increasing $Q_0$ (=3000, 5500, 10 000, and 50 000) of the cavity. The QD starts to enter the strong-coupling regime at $Q_0\approx 5500$. In transmission the formation of the pronounced splitting can be observed. For comparison, the single peaked solid curve shows the transmissivity with no QD present.

$$\Delta\varepsilon_d^{\mathrm{re}}(\omega)=\frac{\Delta\varepsilon_d^0(\omega)}{1-V_d\Delta\varepsilon_d^0(\omega)\mathbf{n}_d\cdot\mathbf{K}(\mathbf{r}_d,\mathbf{r}_d,\omega)\cdot\mathbf{n}_d}.\tag{3}$$

Here, $V_d$ is the QD volume, $\Delta\varepsilon_d^0$ the solution for a bare QD in the presence of electron-phonon scattering, addressed below, and $\mathbf{n}_d$ is the unit vector in direction of the QD dipole moment. Since the latter is usually measured experimentally first to be aligned maximally with the cavity mode (here in $y$ direction, hence $\mathbf{n}_d=\mathbf{e}_y$), we get the dominant component (cavity contribution) for the dot location $\mathbf{r}_d$ at the field antinode position as $K_{yy}(r_d,r_d,\omega)=\omega_{\mathrm{NC}}^2/\{V\varepsilon_b[\omega_{\mathrm{NC}}^2-\omega^2-i\omega(\Gamma_{\mathrm{NC}}+\Gamma_{\mathrm{NC}}^0)]\}$. The effective mode volume is $V$ and $\varepsilon_b$ is the background relative permittivity of the QD host material. Finally, we also obtain the vertically scattered light emission at some arbitrary detector position $\mathbf{R}$, from

$$|E_{\mathrm{vert}}(\mathbf{R})|^2=|V_d\mathbf{G}(\mathbf{R},\mathbf{r}_d,\omega)\cdot\mathbf{n}_d\Delta\varepsilon_d^{\mathrm{re}}(\omega)|^2,\tag{4}$$

emphasizing the important role of the propagator $\mathbf{G}(\mathbf{R},\mathbf{r}_d,\omega)$, which is proportional to $\mathbf{K}(\mathbf{r}_d,\mathbf{r}_d,\omega)$ near the PC nanocavity. The dot product ensures that the directional dependence of the QD dipole moment is taken into account, which should be optimally aligned with the polarization of the target cavity mode.

## III. CONSTANT DEPHASING RATE MODEL

We briefly discuss the results of Eq. (2) for the bare permittivity $\Delta\varepsilon_d^0$ including a phenomenological dephasing constant $\gamma_0$ instead of a microscopically derived phonon mediated decay: $\Delta\varepsilon_d^0=|d_{12}|^2[2V_d\varepsilon_0\hbar(\omega_d-\omega-i\gamma_0/2)]^{-1}$. Here $\omega_d$ is the resonance energy of the QD electron-hole pair, including a homogeneous vacuum Lamb-shift (arising from $\mathrm{Re}[\mathbf{G}(r_d,r_d,\omega)]$), and $d_{12}$ is the corresponding dipole moment. Simulations are shown in Fig. 2. For a NC and QD having the same resonance frequency, the vertical light emission features a spectral splitting of the degenerate systems due to the electron-light interaction—vacuum Rabi splitting (VRS)—of $2\Omega$ with $\Omega=|d_{12}|E_{\mathrm{vac}}/\hbar$, where the term $E_{\mathrm{vac}}=[\hbar\omega_d/(2\varepsilon_0\varepsilon_b V)]^{1/2}$ is often referred to as vacuum-field amplitude. To actually see the spectral splitting, both the line-

widths of the QD and NC must be narrower than the VRS of $2\Omega$. Since the VRS $\Omega$ is a measure for the coupling strength, the QD is in the so-called strong-coupling regime when a splitting is observed.[22] In this context, note that single-QD VRS differs from many-atom VRS found for quantum wells in Fabry-Pérot microcavities.[22,23] To distinguish true strong-coupling and many-atom VRS, the latter is often termed normal-mode splitting.

With a coupling quality factor of $Q_c=6000$ and a cavity quality factor of $Q_0=10\,000$, a clear VRS splitting and a splitting in transmission $|t(\omega)|^2$ is visible (cf. Fig. 2). Further increasing $Q_0$ does not lead to new spectral features but simply to a more pronounced double peak structure. Although extremely high quality factors up to several hundred thousands have been demonstrated recently,[21] we will restrict ourselves to $Q_0=50\,000$. We note already that while the transmission exhibits two distinct peaks at $Q_0=5500$, the corresponding emission shows no splitting at all. Clearly, by comparison of Figs. 2(a) and 2(b), it can be seen that the applicability of transmission spectra for observing the true strong-coupling regime (VRS in $|E_{\text{vert}}|^2$) is limited since splitting in the transmission is not necessarily VRS in the response $|E_{\text{vert}}|^2$ [cf. Eq. (4)]. A more detailed discussion is found at the end of the next section.

## IV. ELECTRON-PHONON SCATTERING

To obtain a microscopical model for the dephasing adjusted in Fig. 2 by a simple time "$T_2$", we now focus on the bare QD dielectric function $\Delta\varepsilon_d^0$ in the presence of electron-phonon scattering. To account for the major dephasing mechanism in QDs with well separated quantum confined energy states, we include the coupling to incoherent bulk phonons. In particular the interaction of the QD electrons with longitudinal-acoustic (LA) phonons via deformation-potential coupling[9,12,25] is considered. The bare permittivity $\Delta\varepsilon_d^0$ can be calculated from the macroscopic polarization $\mathbf{P}$ and the driving electric field $\mathbf{E}$, through $\mathbf{P}(\omega)=\varepsilon_0\Delta\varepsilon_d^0(\omega)\mathbf{E}(\omega)$, where $\mathbf{P}$ is determined from the dipole moment $\mathbf{d}_{12}$ of the confined electron-hole transition, weighted by the density-matrix elements $\rho_{12}$: $\mathbf{P}(t)=V_d^{-1}[\mathbf{d}_{12}\rho_{12}(t)+\mathbf{d}_{21}\rho_{21}(t)]$. Electron-LA phonon scattering leads to "pure dephasing" of the coherent polarization. For a single excitonic level and a phonon bath, the theoretical model system (IBM) can be solved exactly and phonon processes up to infinite order are taken into account. Excitation with a $\delta$ pulse leads to an analytic expression for the phonon-induced temporal decay of the polarization[10,12] given by

$$\rho_{12}(t)=\rho_{12}(0)\exp\left\{\left(-i\omega_d-\gamma_{\text{ZPL}}+i\sum_{\mathbf{q}}\frac{|g_{vc}^{\mathbf{q}}|^2}{\hbar^2\omega_{\mathbf{q}}^2}\right)t-\sum_{\mathbf{q}}\frac{|g_{vc}^{\mathbf{q}}|^2}{\hbar^2\omega_{\mathbf{q}}^2}[n_{\mathbf{q}}e^{i\omega_{\mathbf{q}}t}+(n_{\mathbf{q}}+1)e^{-i\omega_{\mathbf{q}}t}]\right\}. \quad (5)$$

For the LA phonons we consider a coupling via the deformation potential with the electron-phonon coupling element[10] $g_{vc}^{\mathbf{q}}$. The temperature $T$ thus enters via the thermal Bose distribution $n_{\mathbf{q}}(T)$ and $\omega_{\mathbf{q}}$ is the corresponding LA phonon dispersion with wave number[26] $\mathbf{q}$.

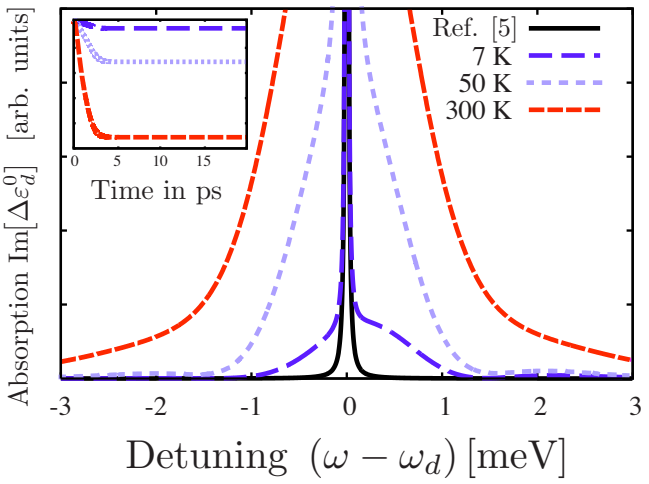


FIG. 3. (Color online) The absorption of a GaAs QD in a homogeneous medium for different temperatures ($T=7$, 50, and 300 K). Compared are calculations of the QD permittivity in Ref. 5 (solid line) and the IBM (dashed lines). The typical parameters are $\hbar\omega_d=1.5$ eV for the QD gap frequency and $d_{12}=50$ D for the dipole moment. The narrow ZPL on top of the phonon sidebands is broadened by a damping ranging between 630–6 ps in agreement with experiments (Ref. 24). For $T=7$ K, the typical asymmetry in the absorption due to spontaneous phonon emission can be seen. The inset shows the temporal evolution of the QD's polarization $P$ with two distinct time scales: a fast initial phonon-induced decay within picoseconds and a very slow radiative decay on a nanosecond time scale.

The QD spectral absorption $\alpha(\omega)\propto\text{Im}[\Delta\varepsilon_d^0]$ can be numerically obtained by a Fourier transform of Eq. (5), shown in Fig. 3. In contrast to the previously used purely Lorentzian QD permittivity by Hughes and Kamada,[5] we obtain, besides the spectrally very sharp Lorentzian zero-phonon line (ZPL), nontrivial broad sidebands due to (i) the dispersion of the involved LA phonons for low temperatures and (ii) nonradiative dephasing at elevated temperatures (50 and 300 K). The broadening of the ZPL is added by a phenomenological dephasing $\gamma_{\text{ZPL}}=\gamma_{\text{rad}}+\gamma_{\text{nonrad}}$, accounting for experimental results of Borri *et al.*[24] These ZPL broadening mechanisms, e.g., due to anharmonicity effects,[25,27] phonon scattering from interfaces,[28,29] or modified phonon spectrum[30] leading to $\gamma_{\text{nonrad}}$ are widely discussed in the literature.

Using the results of Fig. 3, we can now calculate the renormalized QD permittivity $\Delta\varepsilon_d^{\text{re}}$ [Eq. (3)] and subsequently investigate the role of electron-phonon scattering on the complete-system spectra [scattered light $|E_{\text{vert}}|^2$ and transmissivity $|t(\omega)|^2$], as shown in Figs. 4(a) and 4(b). At low temperatures (7 K), the familiar VRS of $2\Omega$ is seen for both $|E_{\text{vert}}|^2$ and $|t(\omega)|^2$. The spectra are slightly asymmetric (lower for positive detuning) even for 7 K. This is due to the asymmetric phonon sidebands in the QD susceptibility caused by spontaneous phonon emission, allowing optical absorption energetically above the QD resonance and subsequent emission of a phonon. With rising temperature (blue to red), the interaction of the dipole transition with acoustical phonons, as well as the ZPL dephasing, increases. Consequently, each peak is further broadened, causing the peak height to drop and ultimately the VRS in $|E_{\text{vert}}|^2$ vanishes

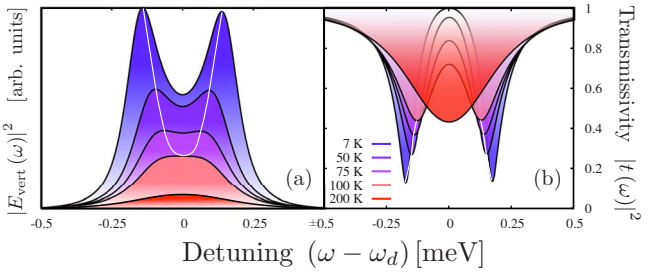


FIG. 4. (Color online) (a) Temperature dependence of the VRS for $Q_0$=50 000 and $Q_c$=6000, including electron-phonon coupling as well as temperature-dependent ZPL. The vanishing VRS shows that the strong-coupling regime is left at approximately 100 K although it remains a clear splitting in (b) the transmission spectra $T(\omega)$. Finally, at room temperature, both spectra clearly lack of VRS. Note the slight asymmetry of the peak heights even for very low temperatures. The white line is a guidance for the eye to emphasize the peak position.

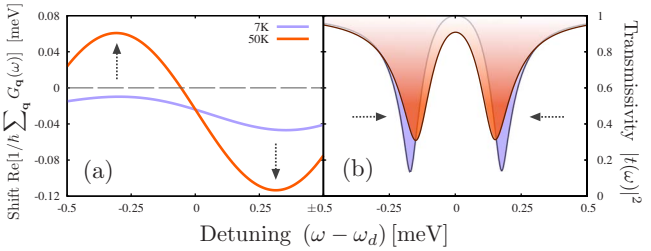


FIG. 5. (Color online) (a) Phonon induced renormalization of the resonance frequency for 7 and 50 K. The gray line marks zero shift. Below (above) the QD resonance, a positive (negative) shift is found. (b) Corresponding transmission spectra featuring a narrower VRS with higher temperature.

above 100 K [cf. Fig. 4(a)]. Interestingly, from Fig. 4(b), the waveguide transmission maintains two characteristic peaks even when dephasing above 100 K is strong. In both spectra, the observed dip becomes spectrally narrower than $2\Omega$ at elevated temperatures. Next, we discuss both observations [dip narrowing (i) and the transmission dip (ii) remaining at elevated temperatures].

(i) In order to get a better insight into the influence of the phonon bath on the spectra especially the transmission gap narrowing for higher temperatures, we consider an analytic limit: Derived via the equations of motion in correlation expansion for a one-phonon process only, it is possible to find an analytic solution in the linear limit[10,31] for the polarization $\rho_{12}(\omega)$. In Fourier space it is given by

$$\rho_{12}(\omega) = \Omega(\omega) \Big/ \left[ \omega_d - \omega - i\gamma_{\text{ZPL}} - \frac{1}{\hbar^2} \sum_{\mathbf{q}} G_{\mathbf{q}}(\omega) \right]. \quad (6)$$

The material response to an incident field $E$, included here in the Rabi frequency $\Omega(\omega) = |d_{12}|E(\omega)/\hbar$, is basically given by a Lorentzian, as used for the dephasing rate model to include the ZPL linewidth.[25] In addition the sum in the denominator of Eq. (6) (a superposition of phonon-induced Lorentzians for occurring virtual processes) gives rise to a non-Lorentzian line shape of $\rho_{12}(\omega)$. The imaginary part of the sum,

$$\sum_{\mathbf{q}} G_{\mathbf{q}}(\omega) = \sum_{\mathbf{q}} |g_{vc}^{\mathbf{q}}|^2 [(n_{\mathbf{q}} + 1)/(\omega_d - \omega + \omega_{\mathbf{q}} - i\gamma_{\text{ZPL}}) + n_{\mathbf{q}}/(\omega_d - \omega - \omega_{\mathbf{q}} - i\gamma_{\text{ZPL}})],$$

contributes to the dephasing leading to $\gamma(\omega, T)$, whereas the real part gives a frequency-dependent shift of the oscillator strength due to the electron-phonon interaction induced self-energy. The latter is shown in Fig. 5. Since this simple analytic model of a correlation expansion up to second order (one-phonon process) fails for temperatures above 50 K,[10,12] results for higher temperatures are not shown. Still a very clear trend can be seen: For negative (positive) detuning, the line shift is toward higher (lower) energies. It becomes more pronounced for elevated temperatures. Therefore we attribute the VRS narrowing to self-energy shifts induced by the electron-phonon interaction. Within the full IBM where an infinitive number of phonon processes is included, this effect is enhanced. Due to the shift in opposite direction, the splitting in both $|t(\omega)|^2$ as well as in the vertically scattered light emission narrows with rising $T$.

(ii) The observed transmission splitting narrower than $2\Omega$ for higher temperatures in weak coupling (for vanishing VRS in the scattered light) suggests that another physical process is involved at these temperatures: Our results are in agreement with phenomenological results of Waks and Vuckovic,[6] where a similar effect was observed for a dipole placed in a drop-filter cavity. They show in detail that a splitting in the transmission does not require VRS in the strong-coupling limit because transmission splitting can be understood as an interference effect within a three-level system: A WG-NC-QD system can be mapped on the problem of electromagnetically induced transparency,[32] where spectral dips are due to destructive interference from the coherent coupling within a three-level system for parameter ranges in the weak-coupling limit. For a detailed analysis, we refer to Ref. 32.

Analyzing the scattered light emission and transmission, it is obvious that caution must be exercised when assuming that transmission spectra give any true signature of the strong-coupling regime.

Nevertheless, as shown recently, the spectral dips in transmission on its own offer some unique light-matter transmission control such as very slow and fast light regimes,[33] and that the qualitative and quantitative effects of electron-phonon scattering should be considered.

## V. CONCLUSION

To conclude, a theoretical formalism that accounts for both electron-phonon and electron-light interaction for the WG transmission within "all-integrated" PC chip has been presented. Our approach allows one to explore the temperature dependence of both the VRS between NCs and the optical properties of embedded single QDs in a straightforward manner. Most notable we predict that strong coupling in emission is lost for temperatures of about 100 K and a shrinking of the VRS with increasing temperature. In an experiment this regime may be left at even lower temperatures

due to other dephasing mechanisms, e.g., impurity scattering or ionization of the QD electron. Depending on the details of the cavity, an interference splitting of the light transmission survives up to much higher temperatures, leaving the WG highly transparent at the dipole resonance frequency, which is important for slow light applications and light propagation control.

**ACKNOWLEDGMENTS**

We thank A. Badolato for useful comments. This work was financially supported by the Deutsche Forschungsgemeinschaft within the Sfb 787, the Natural Sciences and Engineering Research Council of Canada, and the Canadian Foundation for Innovation.

*frank@itp.physik.tu-berlin.de

[1] Y. Akahane, T. Asano, B.-S. Song, and S. Noda, Nature (London) **425**, 944 (2003).
[2] T. Yoshie, A. Scherer, J. Hendrickson, G. Khitrova, H. M. Gibbs, G. Rupper, C. Ell, O. B. Shchekin, and D. G. Deppe, Nature (London) **432**, 200 (2004).
[3] A. Badolato, K. Hennessy, M. Atatüre, J. Dreiser, E. Hu, P. M. Petroff, and A. Imamoğlu, Science **308**, 1158 (2005).
[4] K. Hennessy, A. Badolato, M. Winger, D. Gerace, M. Atatüre, S. Gulde, S. Falt, E. L. Hu, and A. Imamoğlu, Nature (London) **445**, 896 (2007).
[5] S. Hughes and H. Kamada, Phys. Rev. B **70**, 195313 (2004).
[6] E. Waks and J. Vuckovic, Phys. Rev. Lett. **96**, 153601 (2006).
[7] M. Kira, F. Jahnke, W. Hoyer, and S. W. Koch, Prog. Quantum Electron. **23**, 189 (1999).
[8] C. Gies, J. Wiersig, M. Lorke, and F. Jahnke, Phys. Rev. A **75**, 013803 (2007).
[9] B. Krummheuer, V. M. Axt, and T. Kuhn, Phys. Rev. B **65**, 195313 (2002).
[10] J. Förstner, C. Weber, J. Danckwerts, and A. Knorr, Phys. Status Solidi B **238**, 419 (2003).
[11] A. Vagov, V. M. Axt, and T. Kuhn, Phys. Rev. B **66**, 165312 (2002).
[12] J. Förstner, C. Weber, J. Danckwerts, and A. Knorr, Phys. Rev. Lett. **91**, 127401 (2003).
[13] K. J. Ahn, J. Förstner, and A. Knorr, Phys. Rev. B **71**, 153309 (2005).
[14] I. Wilson-Rae and A. Imamoğlu, Phys. Rev. B **65**, 235311 (2002).
[15] G. Cui and M. G. Raymer, Phys. Rev. A **73**, 053807 (2006).
[16] G. Mahan, *Many-Particle Physics* (Plenum, New York, 1981).
[17] S. Hughes, L. Ramunno, J. F. Young, and J. E. Sipe, Phys. Rev. Lett. **94**, 033903 (2005).
[18] W. Vogel, D. Welsch, and S. Wallentowitz, *Quantum Optics An Introduction*, 2nd ed. (Wiley, Berlin, 2001).
[19] S. Hughes, Phys. Rev. Lett. **98**, 083603 (2007).
[20] M. Wubs, L. G. Suttorp, and A. Lagendijk, Phys. Rev. A **70**, 053823 (2004).
[21] E. Weidner, S. Combrie, N.-V.-Q. Tran, A. D. Rossi, J. Nagle, S. Cassette, A. Talneau, and H. Benisty, Appl. Phys. Lett. **89**, 221104 (2006).
[22] G. Khitrova, H. M. Gibbs, M. Kira, S. W. Koch, and A. Scherer, Nat. Phys. **2**, 81 (2006).
[23] C. Weisbuch, M. Nishioka, A. Ishikawa, and Y. Arakawa, Phys. Rev. Lett. **69**, 3314 (1992).
[24] P. Borri, W. Langbein, S. Schneider, U. Woggon, R. L. Sellin, D. Ouyang, and D. Bimberg, Phys. Rev. Lett. **87**, 157401 (2001).
[25] E. A. Muljarov and R. Zimmermann, Phys. Rev. Lett. **93**, 237401 (2004).
[26] LA phonon dispersion $\omega_{\mathbf{q}}=c_s|\mathbf{q}|$, and phonon coupling element $|g^{\mathbf{q}}_{vc}|=|g^{\mathbf{q}}_{vv}-g^{\mathbf{q}}_{cc}|$, where $g^{\mathbf{q}}_{ii}=\sqrt{\frac{\hbar q}{2\rho cV}}D_i e^{-q^2\hbar/4m_i\omega_i}$. Used parameters: sound velocity of GaAs $c_s=5110$ m/s, deformation potentials $D_v=-4.8$ eV, $D_c=-14.6$ eV, effective electron and hole mass: $m_{\mathrm{el}}=0.067$ and $m_{\mathrm{hl}}=0.45$, and mass density of GaAs $\rho=5370$ kg/m$^3$.
[27] P. Machnikowski, Phys. Rev. Lett. **96**, 140405 (2006).
[28] G. Ortner, D. R. Yakovlev, M. Bayer, S. Rudin, T. L. Reinecke, S. Fafard, Z. Wasilewski, and A. Forchel, Phys. Rev. B **70**, 201301(R) (2004).
[29] S. Rudin, T. L. Reinecke, and M. Bayer, Phys. Rev. B **74**, 161305(R) (2006).
[30] G. Lindwall, A. Wacker, C. Weber, and A. Knorr, Phys. Rev. Lett. **99**, 087401 (2007).
[31] S. Butscher, J. Förstner, I. Waldmüller, and A. Knorr, Phys. Status Solidi B **241**, R49 (2004).
[32] S. E. Harris, J. E. Field, and A. Imamoğlu, Phys. Rev. Lett. **64**, 1107 (1990).
[33] V. S. C. Manga Rao and S. Hughes, Opt. Lett. **32**, 304 (2007).